RSC Publishing Faraday Discussions

Do solid-to-solid polymorphic transitions in DL-norleucine proceed through nucleation?

Journal:	*Faraday Discussions*
Manuscript ID:	FD-ART-11-2014-000214.R1
Article Type:	Paper
Date Submitted by the Author:	01-Dec-2014

Complete List of Authors:	van den Ende, Joost; Radboud University Nijmegen, Institute for Molecules and Materials Smets, Mireille; Radboud University Nijmegen, Institute for Molecules and Materials de Jong, Daniël; Radboud University Nijmegen, Institute for Molecules and Materials Brugman, Sander; Radboud University Nijmegen, Institute for Molecules and Materials Ensing, Bernd; University of Amsterdam, Vant Hoff Institute for Molecular Sciences Tinnemans, Paul; Radboud University Nijmegen, Institute for Molecules and Materials meekes, hugo; Radboud University Nijmegen, Cuppen, Herma; Radboud University Nijmegen, Institute for Molecules and Materials

CREATED USING THE RSC LaTeX PCCP ARTICLE TEMPLATE – SEE www.rsc.org/electronicfiles FOR DETAILS
PAPER www. rsc.org/faraday_d | Faraday Discussions

Do solid-to-solid polymorphic transitions in DL-norleucine proceed through nucleation?

Joost A. van den Ende,[a] Mireille M. H. Smets,[a] Daniël T. de Jong,[a] Sander J. T. Brugman,[a] Bernd Ensing,[b] Paul T. Tinnemans,[a] Hugo Meekes,[a] and Herma M. Cuppen*[a]

Received 10th November 2014, Accepted Xth XXXXXXXXX 20XX
First published on the web Xth XXXXXXXXXX 200X
DOI: 10.1039/c000000x

DL-norleucine is a molecular crystal exhibiting two enantiotropic phase transitions. The high temperature $\alpha \leftrightarrow \gamma$ transition has been shown to proceed through nucleation and growth [Mnyukh *et al., J. Phys. Chem. Solids*, 1975, **36**, 127]. We focus on the low temperature $\beta \leftrightarrow \alpha$ transition in a combined computational and experimental study. The temperature dependence of the structural and energetic properties of both polymorphic forms is nearly identical. Molecular Dynamics simulations and nudged elastic band calculations of the transition process itself, suggest that the transition is governed by cooperative movements of bilayers over relatively large energy barriers.

1 Introduction

The occurrence of polymorphism in molecular crystals, *i.e.*, the ability of a compound to crystallise in different crystal structures, can have important implications in different areas of industry ranging from the food industry[1] to the production of dyes and pharmaceutical products.[2] Since the crystal structure determines several properties such as dissolution rate and solubility of the manufactured product, control over the obtained polymorph and its stability is desired. Transformations between polymorphic forms can be divided in two categories: solvent mediated[3] and solid-to-solid transformations. Examples of the latter category are transformations induced by temperature[4], gas[5], large pressures[6], or grinding[7].

Most strategies to inhibit or induce solid-to-solid transformations are empirical in nature. In the case of transformations in which the parent and daughter phase have similar structures, there is an ongoing debate whether the transformation mechanism involves a cooperative movement of molecules or occurs through nucleation and growth.[8–10]

[a] *Institute for Molecules and Materials, Radboud University Nijmegen, Heyendaalseweg 135, 6525 AJ Nijmegen, The Netherlands. E-mail: h.cuppen@science.ru.nl*
[b] *Van 't Hoff Institute for Molecular Sciences, University of Amsterdam, Science Park 904, 1098 XH Amsterdam, The Netherlands*

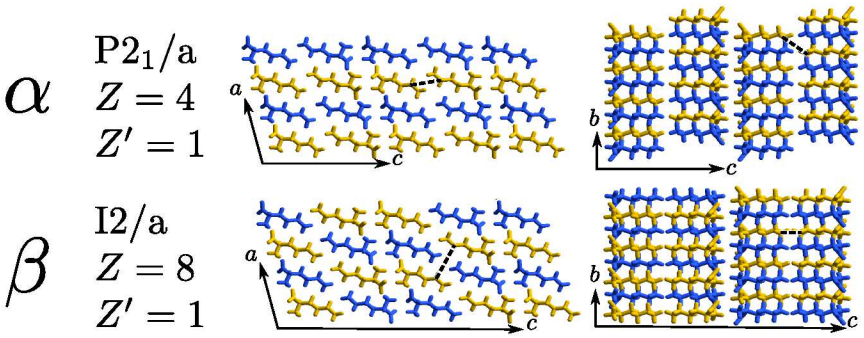

Fig. 1 An overview of the structures of the α and β polymorphic form of DL-norleucine. The molecules are coloured according to their chirality: R-molecules in yellow and S-molecules in blue. The dotted lines depict the distance parameters (DP1 and DP2) which are averaged in-plane distances between molecules of the same chirality in opposing bilayers.

DL-norleucine (2-aminohexanoic acid) is an example of a molecular crystal that exhibits interesting enantiotropic polymorphism, *i.e.*, polymorphism in which the relative thermodynamic stability of the forms changes as a function of temperature in a reversible way. The different polymorphic forms all consist of tightly packed molecular bilayers which are strongly connected by hydrogen bonds between the amino and acid groups. These molecular bilayers are mutually Van der Waals bonded by unbranched hydrophobic side chains.

Mathieson[11] predicted polymorphism to exist for DL-norleucine (DL-NLE) based on X-ray diffraction measurements. More recent determinations of the polymorphic forms β[12] (stable at low temperatures), α[13] (stable at room temperature), and γ[14] (stable at high temperature) confirmed and extended his ideas. The β and α forms consist of highly similar structures in which the molecular conformations are nearly identical.[15] Figure 1 shows the structure of both polymorphs projected along the *b* and *a* axes. The molecules are coloured according to their handedness: R-norleucine is yellow and S-norleucine is blue. The difference between the forms is in the relative position of the bilayers.

The temperature of the α ↔ γ transition is well defined. The α and the γ polymorphic forms differ both in the molecular conformation and in the relative position of the bilayers. The relative position of the bilayers is similar for the γ and the β polymorphic forms, their differences are dominated by a change in molecular conformation. The α ↔ γ transition is accompanied by cracking of the crystals due to a discontinuity in the density at the transition.[9,14] In contrast, the transition from the β to the α form is reported to be 'extraordinarily variable' both in behaviour and in transition temperature.[14] It is still an open question which processes govern the onset of the low temperature transition and whether this solid-to-solid transition can be described by a nucleation-and-growth mechanism or not.

A distinct difference between polymorphic transitions occurring through a nucleation-and-growth mechanism and those occurring through a displacive mechanism is the effect of defects on the occurrence of the transition.[9] When the

transitions proceed through a nucleation-and-growth mechanism, they can be induced by defects that can act as centres of nucleation. Contrarily, for transitions with a displacive character, a defect acts as an obstacle for the transition and has the capability to hinder it. The nucleation-and-growth characteristics of the $\alpha \leftrightarrow \gamma$ transition have convincingly been proven on the basis of these arguments by Mnyukh *et al.* [9].

Recently, some of us have reported that both the lattice parameters and the potential energies of the α and β polymorphic form behave identically as a function of temperature in a Molecular Dynamics (MD) simulations study. [16] We conclude that the difference in volume between the experimentally obtained structures [12,13] is a consequence of thermal expansion and not of differences between the polymorphic forms themselves. This continuous behaviour of the crystal properties, suggests the possibility of a transition without a clear nucleation centre which is in accordance with earlier modelling studies on this transition. [17–20] Furthermore, the recent MD simulations showed partial phase transitions from the β to the α polymorphic form, which result in an intermediate structure. [16]

This discussion tries to pin down the mechanism that governs the poorly understood $\beta \leftrightarrow \alpha$ transition by means of a further computational and experimental characterisation of the polymorphic forms and the solid-to-solid polymorphic transition. We use single crystal X-ray diffraction to verify computational results concerning the lattice parameters of the two polymorphic forms. From differential scanning calorimetry results and simulations we deduce energetic properties of the polymorphic forms. To study the mechanism of the transition we use MD simulations with different sizes of the simulation cell. Finally, nudged elastic band calculations are used to probe the energy landscape of the transition.

The outline of the discussion is as follows. Section 2 introduces the properties of the polymorphic forms α and β. In Section 3 we describe our insights concerning the transition mechanism between the polymorphic forms. The main findings and conclusions of these two sections are written in Section 4, followed by the used methodology in Section 5.

2 Polymorphic properties

2.1 Structural properties

Discontinuous behaviour of lattice vectors, angles and/or volume of a crystal as a function of temperature is a sign of a first order phase transition [8,10], which typically occurs through a nucleation-and-growth mechanism. In this discussion we combine experimental (single crystal X-ray diffraction) and modelling (MD simulations) results of the temperature dependence of the lattice parameters of β and α DL-NLE. The usage of MD allows for the study of a polymorphic form even in its metastable regime where experimentally this form might be inaccessible because of its limited lifetime.

Along the lines of our earlier work [16], we have determined the values of the lattice parameters through MD simulations for both the α and β polymorphic forms at a number of temperatures between 120 and 350 K. Figure 2 shows the behaviour of all three lattice vectors, the monoclinic angle and the volume as a function of temperature. For the α polymorphic form we have doubled the unit

cell in the *c* direction to have the same number of molecules in the unit cell as β and to make the forms easily comparable. As one can see, the cell parameters behave identically for the α and β polymorphic form. This implies that all these five properties and their derivatives with respect to temperature, depend on the temperature in a continuous way, thereby allowing the possibility of a transition governed by a displacive mechanism. Notably, the thermal expansion is almost only affecting the *c*-axis, which is perpendicular to the bilayers, and the β-angle.

These results can be compared with the experimental lattice parameters of DL-NLE determined using single crystal X-ray diffraction (SCXRD). The results of such a measurement on a good quality single crystal with a clear $\alpha \rightarrow \beta$ transition is shown in Figure 2. The α phase unit cell was found above 253 K and the β unit cell was found upon cooling for temperatures between 253 K and 113 K. When the crystal was heated again, the β phase was retained until room temperature. However, after leaving the crystal at room temperature for about 60 hours the crystal had spontaneously transformed to the α polymorph.

From Figure 2 it is clear that the lattice parameters and the thermal expansion of α and β are very similar to the results of the MD simulations, apart from an offset. No clear discontinuity is observed in the volume of the unit cell nor in the cell parameters. The inset of the panel for the *c*-axis shows the results of another measurement of the same single crystal with smaller increments in the temperature region of the transition. One can see that only for one specific temperature (253 K) both polymorphic forms were assigned to the obtained diffraction pattern. For this particular crystal, the transition was quite fast and a clear transition temperature could be identified. For other crystals this was not always the case. Typically, there is a temperature regime where diffraction peaks of both phases are present, which indicates coexistence of the α and β phase. This temperature regime can be quite large (even up to 100 K). Subsequent measurements of the same crystal resulted in similar lattice parameters as a function of temperature, but the amount of disorder in the layer stacking upon cooling and the temperature region of the phase transition varied from crystal to crystal. In some measurements extra peaks were visible that indicate disorder in the layer stacking or a super cell in the *c*-direction perpendicular to the layers. In other cases the reflections showed severe streaking. Besides, in some crystals no signs of a phase transition were visible down to 173 K. In summary, the behaviour of the crystals of DL-norleucine is extremely variable and the $\alpha \leftrightarrow \beta$ transition remains difficult to characterise.

The large similarity between the experimental and simulation results, both quantitatively and qualitatively, is reassuring. The fact that in both cases no discontinuities are observed and that the MD reproduces the anisotropy of the thermal expansion tells us that the MD simulations and the applied force field are accurate and this gives confidence that we can use the atomistic information from the simulations to learn more about the mechanism of the transformation.

2.2 Energetic properties

To assess whether the relative experimental stability of the polymorphic forms could be represented by our computational description of the system (see Section 5.4.1), we performed a 0 K geometry optimization. The minimal energies of the

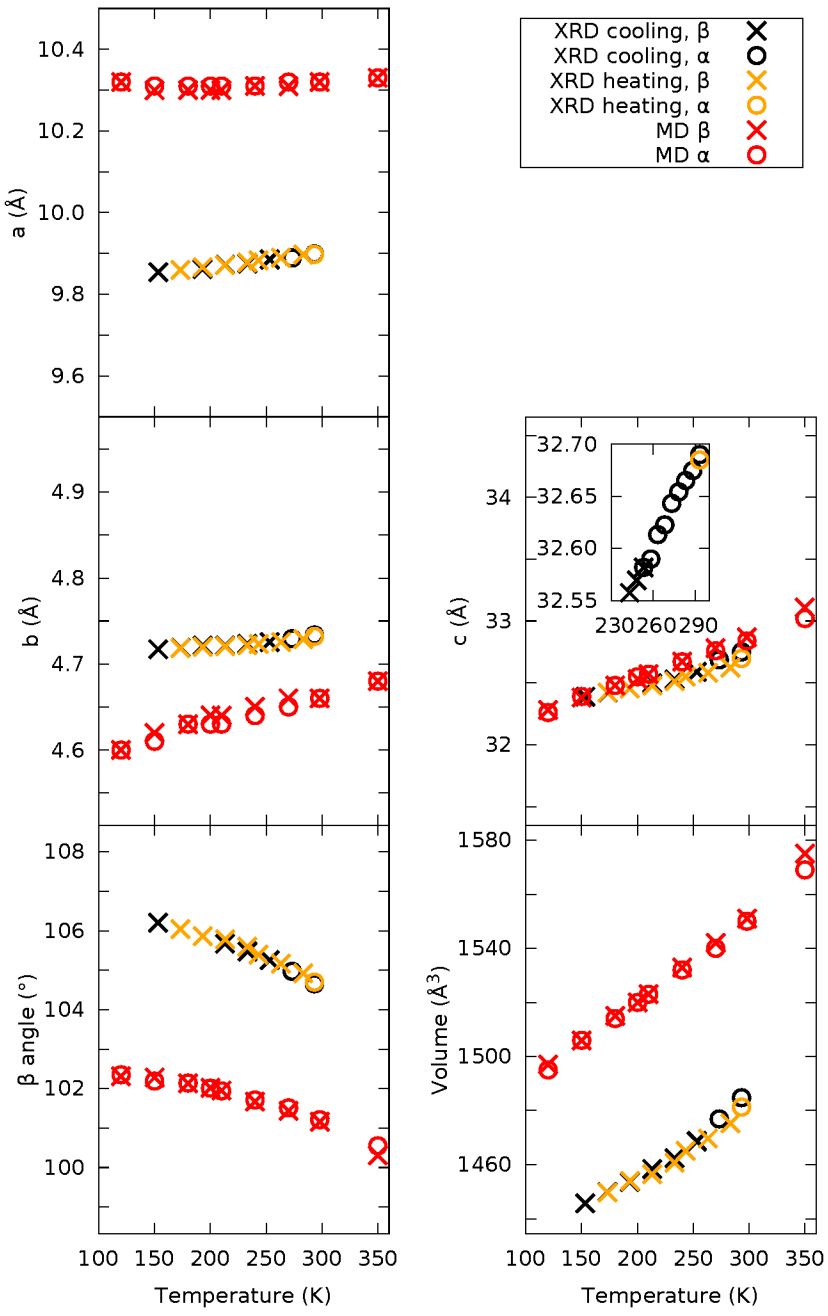

Fig. 2 The lattice parameters of DL-norleucine as a function of temperature as determined using SCXRD and MD simulations. The inset in the c-panel, shows a second measurement of the same single crystal with additional points measured in the temperature range of the transition.

three polymorphic forms are: -93.5 kJ/mol for β, -92.3 kJ/mol for α and -84.6 kJ/mol for γ. The order $\beta < \alpha < \gamma$ agrees with the experimental stability order. The energy difference between the β and α polymorphic form (1.2 kJ/mol) is lower than the available thermal energy at room temperature (2.5 kJ/mol). The difference in energy between the α and γ polymorphic form is clearly higher with 7.7 kJ/mol. Particularly, the small energy difference between the β and α polymorphic form in combination with the large hysteresis in transition temperature, suggests the presence of a relatively large energy barrier for this transition.

Besides the geometry optimization, we have studied the enthalpy of the polymorphic forms as a function of temperature by means of MD simulations. Figure 3 shows the dependence of the enthalpy on temperature. Again, these values are identical for the β and α polymorphic forms at all temperatures. Combined with the information depicted in Figure 2, we conclude that the difference in relative orientation of the molecular bilayers with respect to each other is not a source for an observable enthalpy difference between the polymorphic forms. Moreover, this implies that transitions from β to α or *vice versa*, can occur without a net discontinuity in the enthalpy. An energy barrier between the two phases might still exist.

The heat capacity at constant pressure (C_p) can be obtained from the temperature dependence of the enthalpy. Not surprisingly, these are similar for both polymorphic forms: $C_p(\alpha) = C_p(\beta) = 5.6 \times 10^2$ J/(molK). From this, one can obtain the difference in entropy over the temperature range:

$$S(T_f) - S(T_i) = \int_{T_i}^{T_f} \frac{C_p}{T} dT \approx C_p \ln \frac{T_f}{T_i} = 6.0 \times 10^2 \text{ J/molK},$$

for both polymorphic forms, in which $T_i = 120$ K and $T_f = 350$ K. Since, the reversible polymorphic transition occurs in this temperature range, there must be a finite difference in absolute entropy between the two polymorphic forms at 120 K. An estimate of this difference obtained from a calculation of the crossing of the Gibbs free energies, is:

$$S(\alpha, T_i) - S(\beta, T_i) = (H(\alpha) - H(\beta))/T_{trans} \approx 4 \text{ J/molK},$$

in which T_{trans} is approximated by 300 K. Indeed, the transition is driven by a small entropic difference and moreover, this difference has a very small temperature dependence.

The energetic resemblance of the polymorphic forms is confirmed by differential scanning calorimetry (DSC) results. Certain single crystals show several small exothermic peaks between 254 K and 242 K during cooling (Figure 4), which suggest a very small enthalpy change upon transforming from the α to the β polymorph. For these crystals no peak is observed during the heating process. However, the occurrence of the small peaks upon subsequent cooling indicates that the backward transition must have taken place. The peaks occur typically at slightly different temperatures and have different intensities (≈ 0.02 kJ/mol). Several other crystals show no peak during the cooling and subsequent heating of the crystal below 383 K. In powdered samples of similar weight, which intrinsically contain more defects than single crystals, no enthalpy change is observed. Moreover, after the single crystal undergoes the $\alpha \rightarrow \gamma$ transformation, no peaks were observed in the DSC measurements around 250 K, most probably due to

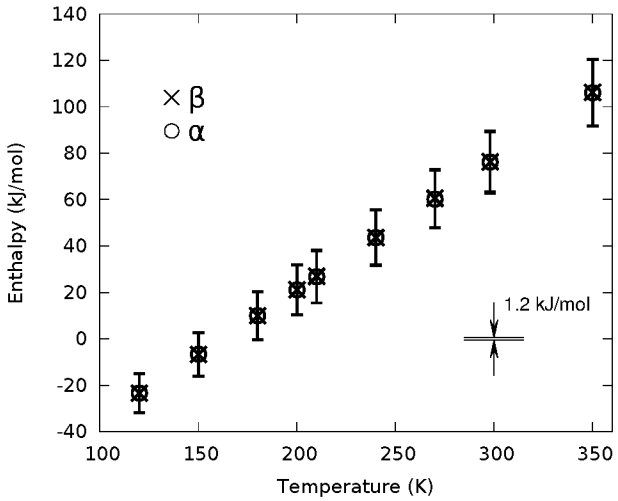

Fig. 3 The enthalpy of the β and α polymorphic forms as obtained from the MD simulations show identical behaviour in their dependence on temperature. The error bars denote the standard deviation of the enthalpy during the simulation, they overlap for both polymorphic forms because the enthalpies show identical behaviour. Crosses denote β and circles denote α. The inset shows the 1.2 kJ/mol lattice energy difference between the polymorphic forms.

cracking of the crystal, which results in more defects. These are arguments against a nucleation-and-growth mechanism for the $\alpha \leftrightarrow \beta$ transition, since in such a mechanism the probability of transitions increases with the amount of defects. On the other hand, the $\alpha \leftrightarrow \gamma$ transition of DL-NLE is clearly observed at 391 K during heating as a strong endothermic peak with a small hysteresis ($\approx$ 2 K) both in powders and single crystals. It has an enthalpy of transition of 4.8 $\pm$ 0.2 kJ/mol in a powdered sample (which is identical to the enthalpy reported in Reference 21) and 4.6 $\pm$ 0.4 kJ/mol in a single crystal, compared to $\approx$ 0.1 kJ/mol for the $\alpha \rightarrow \beta$ transition of a single crystal.

3 Transition mechanism

The β and α polymorphic forms differ from each other by a shift of each second bilayer over *a*/2 and *b*/2, as is depicted in Figure 1. In earlier work we have exploited this difference by introducing two two-dimensional average distance parameters: one in the *bc* plane (DP1) and one in the *ac* plane (DP2). Only distances between molecules of the same chirality are included. For interfaces between the bilayers at the alkane end which have α character, DP1 is roughly 3.5 (high) and DP2 4.5 (low) at 350 K. Interfaces with β character typically have DP1 and DP2 values of 3 (low) and 6.5 (high), respectively. The distance parameters are schematically depicted in Figure 1. In Reference 16 we were able to simulate shifts of individual interfaces from the β (low-high) to an intermediate (high-high) form. Shifts in the perpendicular directions towards (low-low) were never observed (see Figure 8), suggesting an anisotropy in the energy barriers

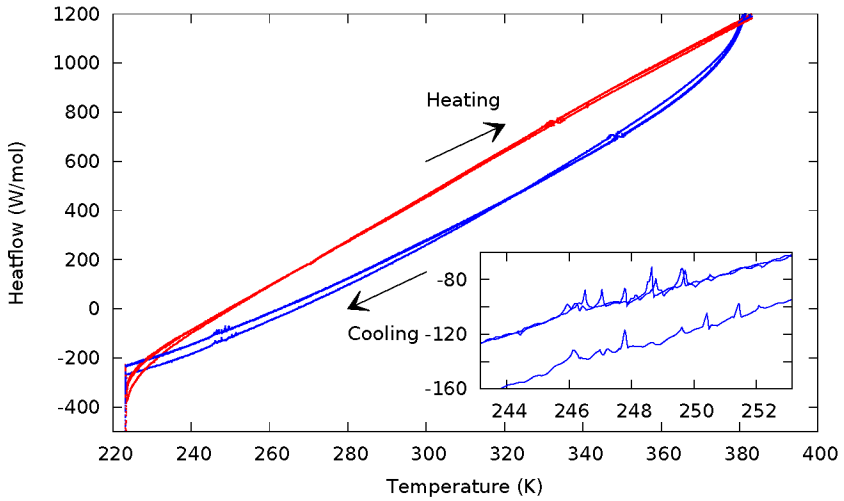

Fig. 4 Three DSC measurements of a single crystal (0.1 mg) between 383 K and 223 K with a heating rate of 2 K/min. Several small peaks indicating the $\alpha \rightarrow \beta$ transition are visible during cooling between 252 K and 244 K (see inset). During heating no peak is observed.

related to this sliding. To extend our insight in the transition mechanism, we present simulations monitored at a higher sampling rate, simulations with different sizes of the simulation cell, and results obtained with the nudged elastic band method[22,23] to probe the different barriers.

3.1 Thermally induced partial phase transitions using MD

One of the observations made in Reference 16 is that the interfaces between bilayers change rather independently of each other. In most of the cases, shifts of bilayers only affected one interface and the extra stress due to a structural mismatch was counteracted by a change in the angle of the simulation cell. Shifts of one bilayer could also result in a change of the local rearrangements of the interfaces on both sides, in which case no volume or angle change of the simulation cell was observed. Since the interfaces can change their character in terms of DP1 and DP2 rather independently, a change of one interface in the simulation cell –which typically has four interfaces– can be seen as a first step in the partial phase transition from β to the intermediate (high-high) form.

Figure 5 shows the change in DP1 and DP2 parameters for such a partial phase transition. In this case, two interfaces are affected, which gives no effective volume change. In previous simulations, the sampling rate was too low to observe intermediate values of DP1. Here we have increased the sampling rate by a factor of ten, which allows us to actually track the transition. Since DP1 and DP2 are parameters depending on an average distance parameter, an intermediate value is not very descriptive. Since it can be the result of a nucleus of molecules which made the full shift and a remaining group of molecules which still needs to follow, or it could be that all molecules are half way, suggesting a cooperative mechanism

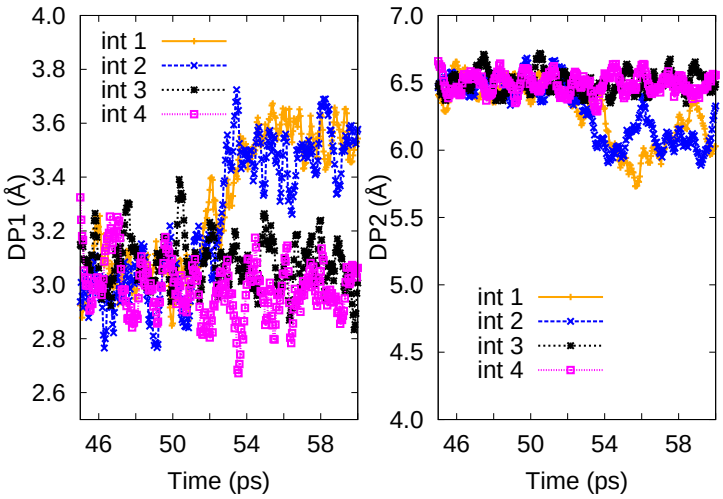

Fig. 5 The time evolution of the two distance parameters during a simulation of the β-polymorphic form at 350 K for the four interfaces of the simulation cell. The changes in DP1 show the partial phase transition along b in which two interfaces are affected. Due to a high sampling frequency of the trajectories, intermediate values for DP1 can be distinguished. A snapshot of the system at intermediate DP1 is shown in Figure 6 for 52.95 ps.

without a clear centre of nucleation.

Figure 6 shows a frame of the MD simulation at 52.95 ps, which is halfway the partial phase transition shown in Figure 5. As one can see, there is no clear centre of nucleation of the transition. All molecules of the most right bilayer move together along the two interfaces in a cooperative manner. This indicates the possible displacive character of the mechanism, at least at the studied length scale of approximately 24 Å.

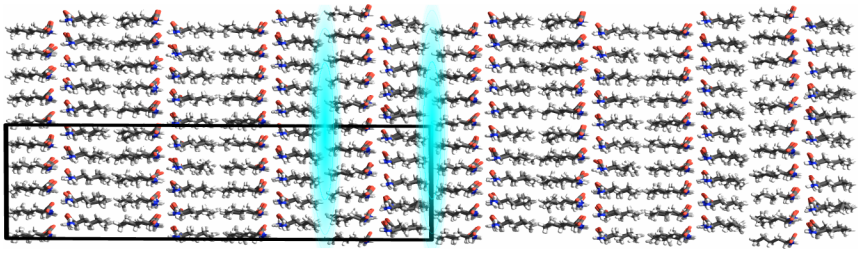

Fig. 6 A snapshot of the *bc*-plane of the MD-simulation halfway (52.95 ps) the partial phase transition that is depicted in Figure 5. There is no clear centre of nucleation of the partial phase transition, since all the molecules in the interfaces (highlighted in cyan) on both sides of the up moving most right bilayer of the simulation cell are halfway between β and α-character. Shown are the R-molecules in the simulation cell projected along *a*. The simulation cell is replicated in the *c*-direction and in the *b*-direction.

3.2 Simulation cell size dependence

To study the influence of the size of the simulation cell on the occurrence of the partial phase transitions, we have performed MD simulations with 14 different simulation cell sizes. For a full treatment of the methodology, we refer to Section 5.4.3. The dimensions are changed along all three directions of the crystal, leading to a change in the size of the bilayers themselves or in the number of bilayers. For all cases periodic boundary conditions are applied and hence the observed size effects are not due to edge effects because the interactions continue over the boundaries of the simulation box. The inverse size dependence of the number of observed partial phase transitionss for the *a*-direction (Figure 7 a) and the *b*-direction (Figure 7 b) is clearly visible. Again, all partial phase transitions occurred along *b*. When the cell size is enlarged along *c*, the number of bilayers grows. This explains the growing number of shifts in Figure 7 c. However, when the transitions are normalised to the number of bilayers, the inverse size dependence is retained (Figure 7 d).

A distinct difference between transitions governed by a nucleation-and-growth mechanism and those having a displacive character, is the dependence on the size of the crystal.[9] The rate of nucleation will increase with size, since there are more possible sites to nucleate, while cooperative motion is harder when more molecules are involved in this cooperative movement. Therefore, the diminishing number of partial phase transitions as a function of the size of the simulation cell could point towards a displacive character of the transition. An alternative explanation for the inverse size dependence of the occurrence of the partial phase

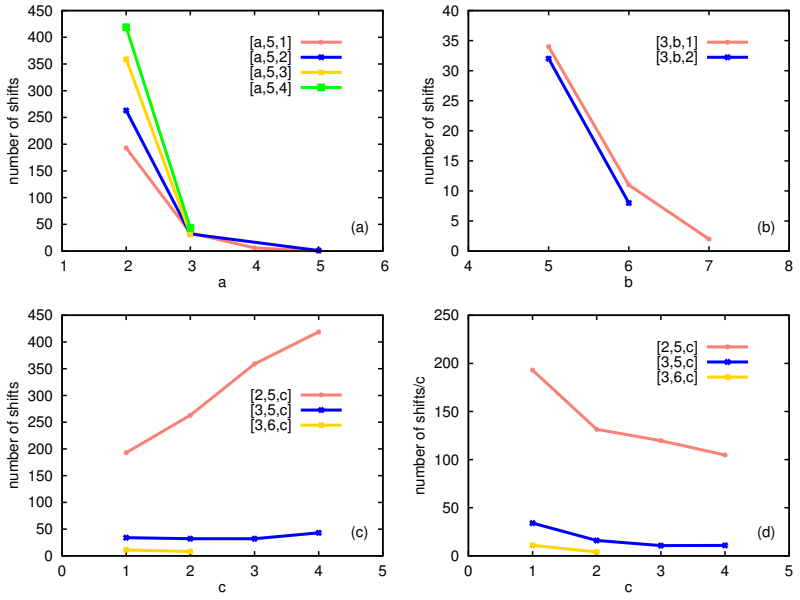

Fig. 7 The number of partial phase transitions in the MD simulations are plotted for different sizes as a function of the number of lattice parameters *a*, *b*, and *c* in the simulation cell (panels a-c). In panel d the number of partial phase transitions is normalized to the number of interfaces through a division by *c* and plotted against *c*. An increase of *a* or *b* (panels a and b) leads to a decrease of the occurrence of partial phase transitions. The same decrease takes place as a function of *c* after the normalization (panel d). These results suggest a displacive character of the partial phase transition.

transitions would be the ratio between the size of the simulation cell and the critical nucleus of the transition in a nucleation-and-growth mechanism. If the simulation cell is too small to sustain the full critical nucleus size, a partial phase transition resulting from a full grown nucleus would be severely hindered. However, the gathering of a few molecules in the process to reach the critical nucleus should be observable, which we never did in our simulations.

3.3 Energy barriers of bilayer shifts

The full scheme of possible transitions for interfaces to go from β character (low-high) to α character (high-low) is depicted in Fig. 8: a direct mechanism in which both shifts occur simultaneously, and two mechanisms in which the transitions occur in a two step fashion with (high-high) and (low-low) as the two possible intermediate forms. By conventional Molecular Dynamics simulations, we have only been able to simulate directly the transition from (low-high) to (high-high), *i.e.*, a slide along *b*. This section presents Nudged Elastic Band calculations (NEB) which give the forward and backward energy barriers for all five processes to check whether the slide along *b* is indeed the most likely transition pathway. For details on the exact usage, we refer to Section 5.4.4.

NEB provides several evaluations of the system along the minimum energy path as well as the transition state structure, given an initial and a final structure. The initial structure in this case is the β form. Because of the implementation of NEB in LAMMPS[24], it is only possible to perform these calculations within the NVT ensemble, and hence no volume changes during the process can be accounted for. For this reason, we have chosen to look at transitions involving the shift of one bilayer, affecting two interfaces instead of a shift of one interface which is accompanied by rearrangements and a volume change of the simulation cell. This is very similar to the process presented in Section 3.1 and hence the results on the (low-high) to (high-high) transition for both cases are directly comparable. The resulting barriers for all back- and forward transitions are calculated by dividing the total energy barrier by the number of molecules in one bilayer and are summarised in Fig. 8. One can see that starting from β the (low-high) to (high-high) transition has indeed the lowest barrier (0.8 kJ/mol), compared to the other possible end states, (low-low, 1.3 kJ/mol) and (high-low, 1.7 kJ/mol). This explains why the shift towards the (high-high) state is the only one which we could probe with MD simulations (denoted in orange in Figure 8).

The use of a fixed simulation cell is a severe limitation in determining the precise values of the energy barriers involved in the shifting of the bilayers. Therefore, the absolute values of the barriers should not be taken to strict. This could be the reason for the difference in the value of the barrier to (high-high) when compared to the 3.0 kJ/mol obtained with a transition path sampling study.[20] However, the relative sizes of the energy barriers related to the different shifts can be deduced from these results and can point at the most likely transition.

Contrary to our earlier suggestion based on the observed partial phase transitions that a transition from β to α would proceed with a shift along *b* followed with a shift along *a*[16], the most likely mechanism for the transition proceeds in the reverse order. The two-independent-shifts picture still holds, but the (low-low) conformation is the most likely intermediate structure, since the process involving the (low-low) conformation has the lowest maximum energy barrier (1.3 kJ/mol) along all three possible pathways which end in the (high-low) conformation. The second step from (low-low) to (high-low) has a much smaller barrier of 0.1 kJ/mol. Please note that the state (high-low) has α-character for 2 out of the 4 simulated interfaces of bilayers, which means that it is not completely the α polymorphic form.

4 Conclusions

This discussion is a contribution to the debate about the possible mechanisms governing solid-to-solid polymorphic transitions in molecular crystals. The possibility or impossibility of cooperative motion to be such a mechanism instead of nucleation and growth of the new phase, is at the heart of this debate. We have studied both computationally and experimentally the low temperature enantiotropic β ↔ α polymorphic transition of the amino acid DL-norleucine. We observe an identical behaviour in the temperature dependence of the lattice parameters for both polymorphs, both with X-ray diffraction measurements and in Molecular Dynamics simulations. The same identical behaviour of the two polymorphic forms is found for the temperature dependence of the enthalpy as

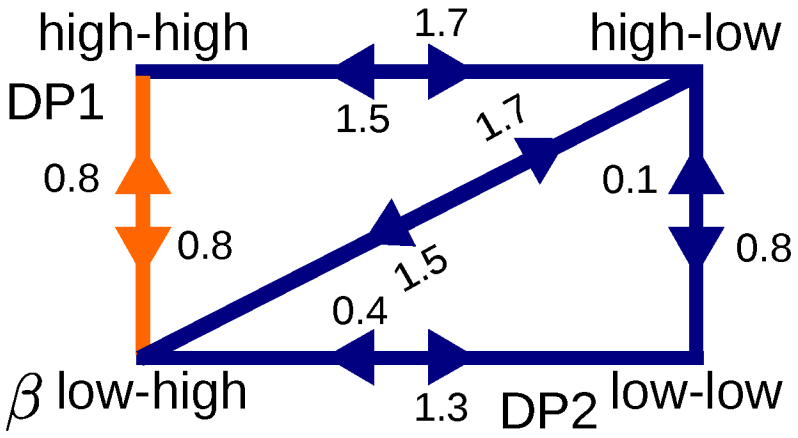

Fig. 8 A schematic overview of the shifts along *b* (DP1) and *a* (DP2) and their energy barriers in kJ/mol DL-norleucine molecules obtained from Nudged Elastic Band calculations. Starting from the β-polymorphic form (low-high) a bilayer has been shifted first along *b* and then along *a* or *vice versa* or shifted along *b* and *a* simultaneously. The end state is (high-low) in which 2 out of the 4 interfaces possess α-character. The transitions from (low-high) to (high-high), which could be probed directly in MD simulations, are depicted in orange. This process has indeed the lowest energy barrier. The most likely path from (low-high) to (high-low) goes via (low-low).

obtained from MD simulations. These similarities in enthalpy are confirmed by differential scanning calorimetry measurements that show only very small peaks upon cooling and no peaks upon heating up to the $\alpha \leftrightarrow \gamma$ transition temperature. This identical behaviour in the properties of the polymorphic forms might point to a concerted or cooperative mechanism.

The congruence between experimental and computational results both in energetic and structural properties, shows the relevance of MD simulations used as a computational microscope to study the transitions on a molecular level. In MD simulations at a high sampling frequency of the trajectories, we did not observe a clear centre of nucleation when zooming in at a partial phase transition along the *b*-axis. There was also no sign of a centre of nucleation in our simulations with different sizes of the simulation cell. On the basis of nudged elastic band calculations we obtained the most likely mechanism of the transition, which is first sliding along the *a*-axis followed by a shift along the *b*-axis.

In summary, the answer to the question of the title of this paper is two-fold. For the high-temperature transition $\alpha \leftrightarrow \gamma$, the answer is definitely "yes" as is proven by Mnyukh *et al.* [9]. This discussion studies the other, $\beta \leftrightarrow \alpha$, polymorphic transition of the compound at lower temperatures. On the basis of our findings we conclude that it is very likely that the polymorphic transition proceeds through a cooperative mechanism with an energy barrier instead of through nucleation and growth.

5 Methodology

5.1 Materials

DL-norleucine (98% pure) was purchased from Alfa Aesar and recrystallised by vapour diffusion from an ethanol/water mixture to form single crystals.

5.2 Differential scanning calorimetry (DSC)

A Mettler Toledo DSC822^e calorimeter in combination with a Julabo FT900 immersion cooler, a TSO 801RO Sample Robot and STAR^e software 11.0 was used for differential scanning calorimetry measurements. Powder samples and single crystals of DL-norleucine have been investigated with this method using heating and cooling rates of 2 to 10 K/min in the temperature range of 223 to 423 K. Samples of a few milligrams were sealed in an aluminium pan (40 μL) and the heat flow was measured in comparison to an empty reference pan. The calorimeter was calibrated with the melting points of indium ($T_{on} = 429.5$ K and $\Delta H = -28.13$ J/g) and zinc ($T_{on} = 692.85$ K and $\Delta H = -104.77$ J/g), both supplied by Mettler Toledo.

5.3 Single crystal X-ray diffraction (SCXRD)

A DL-norleucine single crystal of (0.6x0.2x0.1 mm) was annealed at 383 K for at least 15 min to ensure only the α polymorph was present at the start of the measurements. The crystal was mounted on a goniometer head. Scans for unit cell determination were collected on a Nonius KappaCCD diffractometer in ϕ and ω scan mode using Mo-Kα radiation and a graphite monochromator. The scans were measured at various temperatures during cooling between room temperature and 113 K with a cooling rate of 5 K/min. In addition, at each temperature one scan was collected to observe the changes in the direction perpendicular to the layers of the crystal in more detail during the transition of the α to the β form of DL-norleucine. The unit cell was determined from the scans using the Nonius EvalCCD program suite software[25] and either the α or the β form, or both were chosen. All α unit cells were converted from standard setting $P2_1/c$ to a $P2_1/a$ unit cell with a doubling in the direction perpendicular to the bilayers (c-direction). The β unit cells were converted from a $C2/c$ to an $I2/a$ setting, so that the orientation of the molecules w.r.t. the cell axes of both α and β were comparable.

5.4 Computational Settings

5.4.1 Force Field. The same computational settings for the force field and charges as in Reference 16 are used. In summary, this means the AMBER force field[26] in combination with AM1-BCC charges[27,28]. For the non-bonded interactions a cutoff of 10 Å and an Ewald summation with a precision factor of 10^{-6} were used.

5.4.2 Structures and optimization. LAMMPS[24] was used to obtain the minimal energies of the different polymorphic forms. The experimentally determined structures (DLNLUA01[13], DLNLUA02[12], and DLNLUA05[14]) were minimised

with a convergence of 3.5×10^{-2} kJ/(mol Å) through an appoximated second order method (hftn). To make the cell parameters of the two polymorphic forms easily comparable the same conversion of the settings of the unit cells as described in Section 5.3 was used.

5.4.3 Molecular Dynamics. For a general overview of the issues involved when using MD simulations for studies of molecular crystals we refer to Nemkevich *et al.*[29]. All MD simulations have been performed with DL_POLY_4.05[30] with input files generated with the help of DL_FIELD[31] and GDIS[32]. The anisotropic isothermal-isobaric (NPT) ensemble[33] has been applied with a barostat and thermostat parameter of 0.4 and 0.04 ps, respectively, to simulate at a constant pressure of 1 atm. An integration timestep of 0.5 fs was used. Statistics and trajectories have been recorded every 0.05 and 0.5 ps, respectively. After a three step equilibration process (NVT @ 10 K, NVT @ 120 K (β) or 298 K (α), NPT @ same temperature), 500 ps simulations between 120 and 350 K were performed. All the settings are in accordance with Reference 16.

For the study of the thermal dependence of the polymorphic properties, the simulation cell consisted of 3x5x2 unit cells containing 240 molecules. To study the transition mechanism, 20 different trajectories of 500 ps of the β polymorphic form were simulated at 350 K. This was done for 14 different sizes of the simulation cell: 2x5xc and 3x5xc with c ranging from 1 to 4, 3x6x1, 3x6x2, 3x7x1, 4x5x1, 5x5x1, and 5x5x2 unit cells. For the systems 2x5xc the cutoff radius had to be decreased to 9.8 Å. The occurence of partial phase transitions was followed with the help of two specifically designed distance parameters, which probe the shifts along the planes and are explained in Reference 16.

5.4.4 Nudged Elastic Band. The nudged elastic band calculations[22,23,34] are performed in LAMMPS[24]. The 14 replicas are connected with a spring constant of 1.4 kJ/(mol Å). The time step used in the damped dynamics for the minimisation of the replicas was 0.5 fs. The starting structure (denoted as (low-high) in Figure 8) was a minimised frame of a trajectory without a partial phase transition of an MD simulation of the β polymorphic form at 350 K. From there the other initial structures were obtained by shifting over *b*/2, *a*/2 and *b*/2+*a*/2. In total 12 atoms were connected between the replicas. The atoms (C_α, C_δ, and C_ε) were part of four molecules. These molecules formed two pairs which were located in two interfaces of bilayers. The replicas were minimised with a convergence of the force of 4.5×10^{-2} kJ/(mol Å). The obtained total energy barrier was divided by 60, the number of molecules in one bilayer.

Acknowledgements

H. M. C and M. M. H. S are grateful for support from the VIDI research program 700.10.427, which is financed by The Netherlands Organisation for Scientific Research (NWO). H. M. C, J. A. v. d. E, and M. M. H. S acknowledge the European Research Council (ERC-2010-StG, Grant Agreement No. 259510-KISMOL) for financial support. We thank René de Gelder for stimulating discussions.

References

1 K. Roth, *Chem. Unserer Zeit*, 2005, **39**, 416–428.
2 J. Bernstein, *Polymorphism in Molecular Crystals*, Oxford Science Publications, Oxford, 2002.
3 M. Aucamp, N. Stieger, N. Barnard and W. Liebenberg, *Int. J. Pharm.*, 2013, **449**, 18 – 27.
4 A. Grunenberg, D. Bougeard and B. Schrader, *Thermochim. Acta*, 1984, **77**, 59 – 66.
5 J. Tian, S. J. Dalgarno and J. L. Atwood, *J. Am. Chem. Soc.*, 2011, **133**, 1399–1404.
6 A. Dawson, D. R. Allan, S. A. Belmonte, S. J. Clark, W. I. F. David, P. A. McGregor, S. Parsons, C. R. Pulham and L. Sawyer, *Cryst. Growth Des.*, 2005, **5**, 1415–1427.
7 B. D. Altheimer, S. Pagola, M. Zeller and M. A. Mehta, *Cryst. Growth Des.*, 2013, **13**, 3447–3453.
8 F. H. Herbstein, *Acta Crystallogr. B*, 2006, **62**, 341–383.
9 Y. Mnyukh, N. Panfilova, N. Petropavlov and N. Uchvatova, *J. Phys. Chem. Solids*, 1975, **36**, 127 – 144.
10 J. D. Dunitz, *Pure Appl. Chem.*, 1991, **63**, 177–185.
11 A. M. Mathieson, *Acta Crystallogr.*, 1953, **6**, 399–403.
12 B. Dalhus and C. H. Görbitz, *Acta Crystallogr. C*, 1996, **52**, 1761–1764.
13 M. M. Harding, B. M. Kariuki, L. Williams and J. Anwar, *Acta Crystallogr. B*, 1995, **51**, 1059–1062.
14 S. J. Coles, T. Gelbrich, U. J. Griesser, M. B. Hursthouse, M. Pitak and T. Threlfall, *Cryst. Growth Des.*, 2009, **9**, 4610–4612.
15 U. Mukhopadhyay and I. Bernal, *Mendeleev Commun*, 2004, **14**, 270 – 276.
16 J. A. van den Ende and H. M. Cuppen, *Cryst. Growth Des.*, 2014, **14**, 3343–3351.
17 S. C. Tuble, J. Anwar and J. D. Gale, *J. Am. Chem. Soc.*, 2004, **126**, 396–405.
18 J. Anwar, S. C. Tuble and J. Kendrick, *J. Am. Chem. Soc.*, 2007, **129**, 2542–2547.
19 D. Zahn and J. Anwar, *Chem. Eur. J.*, 2011, **17**, 11186–11192.
20 D. Zahn and J. Anwar, *RSC Adv.*, 2013, **3**, 12810–12815.
21 M. Matsumoto and K. S. Kunihisa, *Chem. Lett.*, 1984, **13**, 1279–1282.
22 G. Henkelman and H. Jónsson, *J. Chem. Phys.*, 2000, **113**, 9978–9985.
23 G. Henkelman, B. P. Uberuaga and H. Jónsson, *J. Chem. Phys.*, 2000, **113**, 9901–9904.
24 S. Plimpton, *J. Comput. Phys.*, 1995, **117**, 1 – 19.
25 A. J. M. Duisenberg, L. M. J. Kroon-Batenburg and A. M. M. Schreurs, *J. Appl. Crystallogr.*, 2003, **36**, 220–229.
26 W. D. Cornell, P. Cieplak, C. I. Bayly, I. R. Gould, K. M. Merz, D. M. Ferguson, D. C. Spellmeyer, T. Fox, J. W. Caldwell and P. A. Kollman, *J. Am. Chem. Soc.*, 1995, **117**, 5179–5197.
27 A. Jakalian, B. L. Bush, D. B. Jack and C. I. Bayly, *J. Comput. Chem.*, 2000, **21**, 132–146.
28 A. Jakalian, D. B. Jack and C. I. Bayly, *J. Comput. Chem.*, 2002, **23**, 1623–1641.
29 A. Nemkevich, H.-B. Burgi, M. A. Spackman and B. Corry, *Phys. Chem. Chem. Phys.*, 2010, **12**, 14916–14929.
30 I. T. Todorov, W. Smith, K. Trachenko and M. T. Dove, *J. Mater. Chem.*, 2006, **16**, 1911–1918.
31 C. W. Yong, DL_FIELD *version 2.2*, http://www.ccp5.ac.uk STFC Daresbury Laboratory, 2012.
32 S. Fleming and A. Rohl, *Z. Kristallogr.*, 2005, **220**, 580–584.
33 G. J. Martyna, M. E. Tuckerman, D. J. Tobias and M. L. Klein, *Mol. Phys.*, 1996, **87**, 1117–1157.
34 A. Nakano, *Comput. Phys. Commun.*, 2008, **178**, 280 – 289.

